Coupled modes with A_1 symmetry in tetragonal $BaTiO_3$

A. Chaves,* R. S. Katiyar,† and S. P. S. Porto
Departments of Physics and Electrical Engineering, University of Southern California, Los Angeles, California 90007
(Received 2 July 1973)

The infrared properties of a system of first-order-coupled phonons are analyzed. The dielectric function and the Raman line shape of the polariton modes are derived. The parameters involved in the theory can be obtained from the Raman spectra of the TO and LO modes or from the Raman spectrum of the TO modes plus infrared-reflectivity measurements. It is shown that we can objectively distinguish real coupling from imaginary, contrary to the current belief. Numerical calculations are performed for the A_1-symmetry modes of tetragonal $BaTiO_3$, with good agreement for the polariton shapes and complete disagreement for the infrared reflectivity; damage at the crystal surface is pointed out as the probable cause of the discrepancy. In addition to the coupling between the lowest and the middle mode, previously known, a much larger coupling between the middle mode and the highest is shown to exist. Both couplings are shown to be real or nearly so. The discrepancy between the dielectric constant created by the resonant modes (electronic plus phonons) and the value obtained by electrical measurements is interpreted as a new indication that the crystal has a dynamical disorder; this disorder could also be cause of an anomalous broadening observed in the lowest polariton.

I. INTRODUCTION

The Hamiltonian of an isolated system can always be brought to a diagonal form, which means that any coupling of the quantum states is reducible. However, no system above the temperature 0 °K is isolated, for we have at least the blackbody radiation connecting it with the environment. Although there is no true stationary state in such a situation, in many cases the interlevel transitions of the system, in the absence of external drive, are so random that the correlation in the dynamics of any two levels is undetectable. A good description of such systems is obtained by just adding a characteristic imaginary component to each element of the diagonalized unperturbed Hamiltonian. In some cases, however, the Hamiltonian of the system is intrinsically nondiagonal. The profile of the energy spectrum of such systems is not composed of a set of Lorentzian peaks, but contains asymmetric interfering features.

Since the occurrence of coupling in the lattice modes was recognized by Barker and Hopfield[1] to explain the infrared reflectivity of some perovskites, a handful of spectral anomalies in data on Raman, Brillouin, and neutron scattering were observed and associated with phonon-phonon coupling.[2-9] As the coupling phenomenon is a temperature-induced effect, it seems probable that its occurrence will be more frequent in crystal showing other thermal anomalies in the phonon behavior. In fact, most of the crystals in which the effect proved to occur, as $BaTiO_3$, $SrTiO_3$, $AlPO_4$, quartz, potassium dihydrogen phosphate (KDP) and cesium dihydrogen arsenate (CsDA), undergo a structural phase transition at some temperature not far from where the interference starts to be observable. $BaTiO_3$ presents three structural phase transitions, at − 80, 6, and 130 °C. In the tetragonal phase between 6 and 130 °C the dynamics of the crystal is complicated. All the three A_1 modes of vibration are strongly coupled and two of them are heavily damped. The lowest optical E mode is overdamped in all that range of temperatures and is coupled with the acoustical modes. Furthermore, the values of both components of the dielectric constant tensor are in disagreement with the values predicted on the basis of the phonon frequencies and infrared strengths. These complications prevented the clear understanding of the mechanism leading to the phase transitions; opinions in the literature are divided concerning important questions, such as whether they are order-disorder or displacive phase transitions.

The A_1 phonons have created some polemic in the past and the question is still not completely answered. The Raman spectrum for the A_1(TO) phonons shows three peaks, two very broad and one (the lowest one) very sharp, but these peaks have many strange properties. One is the striking asymmetry of the lines; another is the permanence of the two broad peaks in the phase above 130 °C, where the O_h symmetry ascribed to the crystal does not allow any first-order Raman scattering. The third difficulty is the failure of the A_1 phonons, if we assign these three peaks as the A_1(TO), to explain the low-frequency value of the dielectric function along the ferroelectric axis. Prior investigators[10,11] interpreted the two broad peaks as coming from second-order scattering, and their interpretation found some support in the fact that most perovskites show strong second-order scattering[12]; but they[10,11] did not pay any attention to the very weak intensity of the peaks for experiments in

the A_1(LO) configuration. Since second-order scattering should be almost direction independent, this comes in contradiction with their interpretation. Pinczuk *et al.*[13] observed that the broad peaks shift to lower frequencies in the polariton region of small wave vectors, an effect expected to occur only with transverse-optical one-phonon levels, and assigned the two bands as A_1(TO). They did not attempt to explain the permanence of the bands in the paraelectric phase. Unfortunately, the measurements of neutron scattering by small-wave-vector phonons in $BaTiO_3$ were limited to energy losses smaller than 25 meV (200 cm^{-1}) and only the lowest A_1(TO), positioned at 178 cm^{-1}, could be observed.[14]

Comes *et al.*,[15] basing their work on the observation of some anisotropic diffuse elastic scattering of x rays in $BaTiO_3$ and $KNbO_3$, proposed that these crystals, and presumably also other perovskites, have a disordered structure. The Ti (or Nb) does not sit on the C_4 axis of the crystal, but at one of eight positions on the body diagonals of the cell. In the paraelectric phase, the eight sites would be equivalent and then the crystal would be cubic on the average. This kind of disorder can explain the permanence of part of the first-order Raman scattering in the paraelectric phase of $BaTiO_3$; being a fast phenomenon, the Raman scattering employs the instantaneous symmetry of the cell instead of the average one. However, it was shown by Huller[16] that the site disorder is not required to explain the anisotropic diffuse scattering of x rays, for the dynamical disorder resulting from the overdamped optical phonon of E symmetry can give the same effect. This view was adopted also by Harada *et al.*[9] to explain a diffuse quasielastic scattering of neutrons by cubic $BaTiO_3$.

In a previous work, we investigated the "mechanical" coupling of the two lowest A_1 polaritons of tetragonal $BaTiO_3$.[17] The electromagnetic coupling of the modes was not considered explicitly; consequently, the dispersion of the polaritons generated a new set of effective parameters for the system at each different angle of scattering. That kind of approach, although very useful in the study of the behavior of the polaritons, cannot give a comprehensive understanding of all the infrared properties of the crystal. In fact, one wants to know if the observed shapes for the polaritons can be explained by the parameters contained in the TO and LO spectra, a question which is left open in that approach. Benson and Mills[18] considered the electromagnetic coupling in their study of the polaritons. However, their work had some limitations that must be overcome if the desired comprehensive view is to be achieved. They chose a set of parameters which was able to give the best explanation of the available data on polaritons; this set was found to be unique. However, according to the current belief, there are infinite sets of parameters which would give exactly the same fitting, and the contradiction is not answered by these investigators. They also did not consider the very large coupling between the second and third A_1-symmetry modes. Finally the coupled-modes model was not applied consistently to the calculation of the mode strengths. In this paper, we evaluate the dielectric function and the Raman line shape of the polaritons, starting from the Raman spectra of the TO and LO modes. Numerical calculations are performed for the A_1 modes of $BaTiO_3$. Some emphasis is given to the discussion on the transformation properties of the system. Previous workers concluded that the formulas for the dielectric function and the Raman line shape were invariant under unitary transformations and used some kind of heuristic criterion to select one particular representation for the coupled-modes system. That invariance is shown to be only apparent and not true for modes which carry electric dipole moment.

II. RESPONSE OF THE CRYSTAL TO EXTERNAL MECHANICAL FORCES

Let the crystal have $3N$ optical modes of vibration, which means that the unit cell has $N+1$ atoms; ϵ_∞ and ϵ_0, respectively, are defined as the optical and static dielectric tensors; the electronic vibrations are represented by a set of three oscillators, each one polarized along one of the principal axes of ϵ_∞. For crystals with orthorhombic or higher symmetries the polarization of the lattice modes is also aligned along the principal axes of ϵ_∞, which implies that ϵ_0 and ϵ_∞ can be diagonalized simultaneously. We will restrict ourselves to these highly symmetric crystals and will introduce couplings between the $3N+3$ modes according to the classical equations below:

$$M_\nu(\ddot{W}_\nu+\gamma_\nu\dot{W}_\nu+\omega_\nu^2 W_\nu)+\sum_{\mu\neq\nu}^{3N}(M_\nu M_\mu)^{1/2}(\gamma_{\nu\mu}\dot{W}_\mu+\omega_{\nu\mu}^2 W_\mu)$$

$$+\sum_{j=1}^{3}(M_\nu m_j)^{1/2}(\gamma_{\nu j}\dot{W}_j+\omega_{\nu j}^2 W_j)+\sum_{j=1}^{3}\alpha_{\nu j}(W_\nu-W_j)^2-Z_\nu\hat{e}_\nu\cdot\vec{E}=F_\nu\,,\quad \nu=1,2,\ldots,3N$$

$$m_j(\ddot{W}_j+\gamma_j\dot{W}_j+\omega_j^2W_j)+\sum_{\mu=1}^{3N}(m_jM_\mu)^{1/2}(\gamma_{j\mu}\dot{W}_\mu+\omega_{j\mu}^2W_\mu)-\sum_{\mu=1}^{3N}\alpha_{j\mu}(W_\mu-W_j)^2-z_jE_j=F_j\,,\quad j=1,2,3\,. \tag{1}$$

In the Eqs. (1), W_ν and W_j are the amplitudes of the motion along each mode; F_ν and F_j are external forces acting on each mode; M_ν, m_j, and Z_ν, z_j are effective masses and effective charges associated with the modes, and E is the electric field induced by the crystal polarization; ν (or μ) labels the $3N$ ionic optical modes and j labels the three oscillators representing the electronic transitions. E is simply the macroscopic field inside the crystal, and the corrections for local fields are included in the effective charges.

The nonlinear coupling between the electrons and the modes is necessary in order for a nonzero Raman effect to occur, but it is too small to affect considerably the response of the set of oscillators to external forces. So, our first step is to make the system linear and evaluate its response function.

We can make the system look simpler with the transformation

$$X_\nu=(M_\nu)^{1/2}W_\nu\,,\quad Q_\nu=(M_\nu)^{-1/2}Z_\nu\,. \tag{2a}$$

This transformation is convenient because the expression for the crystal polarization will stay invariant,

$$\sum W_\nu Z_\nu=\sum X_\nu Q_\nu\,, \tag{2b}$$

and so will the expression for the electric field. The linearized equations (1) will transform to

$$\sum_{\mu=1}^{3N+3}(-\omega^2\delta_{\nu\mu}-i\omega\gamma_{\nu\mu}+\omega_{\nu\mu}^2)X_\mu(\omega,\vec{q})$$

$$-Q_\nu\hat{e}_\nu\cdot\vec{E}(\omega,\vec{q})=f_\nu(\omega,\vec{q})\,, \tag{1'}$$

where the forces have also been transformed: $f_\nu=(M_\nu)^{-1/2}F_\nu$. We have made the convention that $\gamma_{\nu\nu}\equiv\gamma_\nu$, and $\omega_{\nu\nu}\equiv\omega_\nu$, when writing Eqs. (1').

To solve Eqs. (1') we need first the expression for the electric field in terms of the normal-coordinates amplitudes. That expression comes from Maxwell equations

$$\vec{\nabla}\times\vec{E}=-\frac{1}{c}\frac{\partial\vec{B}}{\partial t}\,,$$

$$\vec{\nabla}\times\vec{H}=\frac{1}{c}\frac{\partial\vec{D}}{\partial t}\,,$$

$\vec{D}$ and $\vec{E}$ being connected by

$$\vec{D}=\vec{E}+4\pi\vec{P}=\vec{E}+\sum_{\mu=1}^{3N+3}\hat{e}_\mu X_\mu Q'_\mu\,,$$

where V is the volume of the unit cell. The effective charge Q'_μ defined by this relation cannot *a priori* be identified with Q_μ. Taking $\vec{B}=\vec{H}$, the wave equation gives the following relation:

$$-\vec{q}(\vec{q}\cdot\vec{E})+q^2\vec{E}=(\omega^2/c^2)[\vec{E}+(4\pi/V)\hat{e}_\mu X_\mu Q'_\mu]\,. \tag{3}$$

The three-dimensional matrix $\overleftrightarrow{T}$ is defined by

$$4\pi T_{ij}^{-1}=(q^2c^2/\omega^2-1)\delta_{ij}-(q^2c^2/\omega^2)\hat{q}_i\hat{q}_j\,,\quad \hat{q}_i=q_i/q$$

which means

$$T_{ij}=-4\pi\hat{q}_i\hat{q}_j+\frac{4\pi}{q^2c^2/\omega^2-1}(\delta_{ij}-\hat{q}_i\hat{q}_j)\,. \tag{4}$$

The electric field will be given by

$$E_i=\sum_{j=1}^{3}T_{ij}\frac{1}{V}\sum_{\mu=1}^{3N+3}\hat{e}_j\cdot\hat{e}_\mu X_\mu Q'_\mu\,, \tag{5}$$

where e_μ and e_j are the polarization directions of the modes.

The equations (1') can now be written only in terms of X_ν and f_ν:

$$\sum_{\mu=1}^{3N+3}(-\omega^2\delta_{\nu\mu}-i\omega\gamma_{\nu\mu}+\omega_{\nu\mu}^2)X_\mu$$

$$-\frac{1}{V}\sum_{\mu=1}^{3N+3}\Big(\sum_{i,j=1}^{3}T_{ij}\hat{e}_i\cdot(\hat{e}_\nu\hat{e}_\mu)\cdot\hat{e}_j\Big)Q_\nu Q'_\mu X_\mu=f_\nu\,. \tag{6}$$

It is convenient to group the whole expression multiplying the charges in a short symbol:

$$\Phi_{\nu\mu}(\omega,\vec{q})=\sum_{i,j}^{3}T_{ij}(\omega,\vec{q})\hat{e}_i\cdot(\hat{e}_\nu\hat{e}_\mu)\cdot\hat{e}_j\,; \tag{7}$$

then Eq. (6) becomes

$$\sum_{\mu=1}^{3N+3}(-\omega^2\delta_{\nu\mu}-i\omega\gamma_{\nu\mu}+\omega_{\nu\mu}^2-\Phi_{\nu\mu}Q_\nu Q'_\mu/V)X_\mu=f_\nu\,. \tag{6'}$$

What we were really looking for are the susceptibilities $G_{\nu\mu}$, such that

$$X_\nu(\omega,\vec{q})=\sum_\mu G_{\nu\mu}(\omega,\vec{q})f_\mu(\omega,\vec{q})\,, \tag{8}$$

and Eq. (6') implies

$$G_{\nu\mu}^{-1}(\omega,\vec{q})=-\omega^2\delta_{\nu\mu}-i\omega\gamma_{\nu\mu}+\omega_{\nu\mu}^2-\Phi_{\nu\mu}(\omega,\vec{q})Q_\nu Q'_\mu/V\,. \tag{9}$$

The susceptibility must be invariant to the interchange of parameter indices:

$$G_{\nu\mu}=G_{\mu\nu}\,.$$

This means that

$$\omega_{\nu\mu}=\omega_{\mu\nu}\,,\quad \gamma_{\nu\mu}=\gamma_{\mu\nu}\,,\quad Q_\nu Q'_\mu=Q_\mu Q'_\nu\,.$$

The last relation can be rewritten as

$$Q'_\mu/Q_\mu = Q'_\nu/Q_\nu = \text{const} .$$

A trivial solution to this proportionality is $Q'_\nu = Q_\nu$ for all modes. Huang[19] has shown that this is the only solution compatible with energy conservation.

Some further discussion of the properties of the G matrix shown in Eq. (9) is appropriate. Let us first see how it looks when $\vec{q}$ is parallel to one of the crystallographic axis. In this case, the matrix T is diagonal and consequently $\Phi_{\nu\mu}$ will be zero if the modes ν and μ do not have the same polarization direction. This means that only modes of the same polarization and consequently of the same symmetry will be coupled by their mutual field. Furthermore, we can see that only modes of the same symmetry will be coupled by the harmonicities of the crystal. In fact, the whole potential, and then also its anharmonic part, must have the symmetry of the crystal; this corresponds to saying that the operator that would describe the interaction of modes is a scalar in that symmetry and cannot couple base functions of different irreducible representations of the symmetry group. We can then conclude that $\omega_{\nu\mu}$ and $\gamma_{\nu\mu}$ are zero if the modes ν and μ do not have the same symmetry.

Since modes of different polarization are decoupled, we can, when q goes along one of the crystallographic axes, block-diagonalize the matrix $\overleftrightarrow{G}$. Consider now one such block, to be designated by $\overleftrightarrow{G}_\alpha$. For transverse vibration of these modes, we have

$$G^{-1}_{\alpha\nu\mu}(\omega, q) = -\omega^2\delta_{\nu\mu} - i\omega\gamma_{\nu\mu} + \omega^2_{\nu\mu} - (4\pi/V)(q^2c^2/\omega^2 - 1)^{-1}Q_\nu Q_\mu . \quad (10)$$

Writing Eq. (8) in matrix form

$$\vec{X}_\alpha = \overleftrightarrow{G}_\alpha \vec{f}_\alpha \quad (8')$$

and setting the unitary transformation

$$\vec{X}'_\alpha = \overleftrightarrow{U}\vec{X}_\alpha \quad (11a)$$

$$\vec{f}'_\alpha = \overleftrightarrow{U}\vec{f}_\alpha , \quad (11b)$$

Eq. (8′) will transform to

$$\overleftrightarrow{X}'_\alpha = \overleftrightarrow{U}\,\overleftrightarrow{G}_\alpha\,\overleftrightarrow{U}^\dagger\vec{f}'_\alpha .$$

This means that the G matrix transforms as

$$\overleftrightarrow{G}'_\alpha = \overleftrightarrow{U}\,\overleftrightarrow{G}_\alpha\,\overleftrightarrow{U}^\dagger . \quad (12)$$

Equation (10) implies that the charges transform as

$$\vec{Q}'_\alpha = \overleftrightarrow{U}\vec{Q}_\alpha . \quad (11c)$$

It must be emphasized that the transformation (11c) results from the complete isotropy of the matrix $\Phi_{\nu\mu}$ in the very particular situation considered. In the general case the transformation of the effective charges is complicated.

III. RAMAN SCATTERING

We now examine the interaction of the system with light. The nonlinear coupling of the electrons and the modes will be responsible for changes in the frequencies of light. In addition to higher harmonics of the incident light, it will cause the appearance of sidebands, or the Raman effect. The sidebands are the mixing of the incident frequency with the frequenices of the modes of the system.

The Raman scattering will be proportional to $\langle |p|^2\rangle_{\omega_s}$, the fluctuation of the electric dipole moment of the crystal at the scattering frequency ω_s. This dipole comes only from the electron motion, because the ions are too massive to move at the frequency of visible light. The nonlinearity of Eqs. (1) now becomes essential. We will calculate this dipole moment only for the case in which the laser field is along a given crystallographic axis. Since the electrons are decoupled between themselves, the extensions to oblique phonon can be made following the same method.

Suppose the laser field is given by

$$\hat{k}E_L e^{-i(\omega_L t - q_L x)} . \quad (13)$$

This field will move one of the electrons, which oscillates along z; this electron will also be driven by the induced field of the thermally excited lattice modes, by the "mechanical" forces coming from the coupling with the ions, and by random forces of varied origin. The amplitude of its motion at frequency $\omega_s = \omega_L - \omega$ and wave vector $q_s = q_L - q$ will be dictated by the equation

$$(-\omega_s^2 - i\omega_s\gamma_z + \omega_z^2)X_z(\omega_s) - 2(m_z)^{-1/2}\sum_{\mu=1}^{n}\alpha_\mu[X_z^*(\omega) - X_\mu^*(\omega)][X_z(\omega_L) - X_\mu(\omega_L)] = Q_z E(\omega_s) + f_{\text{therm}}(\omega_s) , \quad (14)$$

where f_{therm} represents the purely random forces. The contribution of f_{therm} to $X_z(\omega_s)$ will give origin to blackbody radiation of the crystal. This is the spontaneous radiation which exists superimposed to the true Raman light, but at temperatures which are not too high; this radiation is negligible. The Raman oscillation of the electron is

$$[-\omega_s^2 - i\gamma\omega_s + \omega_z^2 - \Phi(\omega_s, q_s)Q^2]X(\omega_s) = 2X(\omega_L)\sum_\mu \beta_\mu[X^*(\omega) - X_\mu^*(\omega)]$$

or

$$X(\omega_s)=\frac{2QE_L\sum_\mu \beta_\mu[X^*(\omega)-X_\mu^*(\omega)]}{[-\omega_s^2-i\gamma\omega_s+\omega_z^2-\Phi(\omega_s,q_s)Q^2][-\omega_L^2-i\gamma\omega_L+\omega_z^2-\Phi(\omega_L,q_L)Q^2]}\ .$$

The corresponding electric dipole moment is

$$P(\omega_s)=QX(\omega_s)=C(\omega_L,\omega_s)E_L\sum_\mu \beta_\mu[X^*(\omega)-X_\mu^*(\omega)]\ .$$

The scattered intensity is proportional to the power spectrum of the square of the dipole moment:

$$\frac{\langle|P(\omega_s)|^2\rangle}{E_L^2}=|C|^2\left\langle\left|\sum_\mu \beta_\mu[X(\omega)-X_\mu(\omega)\right|^2\right\rangle$$

$$=|C|^2\left\langle\left|X(\omega)\sum_{\mu=1}^{n}\beta_\mu-\sum_{\mu=1}^{n}\beta_\mu X_\mu(\omega)\right|^2\right\rangle\ . \tag{15}$$

Defining

$$\sum_{\mu=1}^{n}\beta_\mu=-\beta_{n+1}\ ,$$
$$X=X_{n+1}\ , \tag{16}$$

We now have

$$\frac{\langle|P(\omega_s)|^2\rangle}{E_L^2}=|C|^2\left\langle\left|\sum_{\mu=1}^{n+1}\beta_\mu X_\mu(\omega)\right|^2\right\rangle$$

$$=|C|^2\sum_{\nu,\mu}^{n+1}\beta_\nu\beta_\mu\langle X_\nu X_\mu\rangle_\omega\ . \tag{17}$$

All the correlations appearing in Eq. (17) are defined by the temperature and the response function of the system, according to the Nyquist theorem:

$$\frac{\langle|P(\omega_L-\omega)|^2\rangle}{E_L^2}=|C|^2\frac{\hbar}{\pi}[n(\omega)+1]\sum_{\nu,\mu}^{n+1}\beta_\nu\beta_\mu\,\mathrm{Im}G_{\nu\mu}(\omega)\ . \tag{18a}$$

Formula (18a) shows that the Raman efficiency is given by a quadratic form of the imaginary part of the G matrix. The number of independent amplitudes β_ν composing the quadratic form is equal to n, the amplitude which corresponds to the electronic mode is related to those associated with the lattice modes by relation (16).

Defining $\vec{\vec{G}}=\vec{\vec{G}}'+i\vec{\vec{G}}''$, we finally can express the differential Raman cross section in the matrix form

$$\frac{d^2\sigma}{d\Omega\,d\omega}\propto[n(\omega)+1]\vec{\beta}^{\dagger}\vec{\vec{G}}''\vec{\beta}\ , \tag{18b}$$

where $\vec{\beta}^{\dagger}$ is the vector defined by

$$\beta^{\dagger}=\left(\beta_1,\beta_2,\ldots,\beta_n,-\sum_{\mu=1}^{n}\beta_\mu\right) \tag{19}$$

IV. DIELECTRIC FUNCTION

The dielectric function of the system is calculated with a procedure very similar to that used in the evaluation of the response to external mechanical stimuli. The stimulus to be considered now is the total macroscopic field inside the crystal and the response is the total polarization. The electric susceptibility tensor is defined by

$$P_i=\sum_{j=1}^{3}\chi_{ij}E_j^{\mathrm{tot}}\ . \tag{20}$$

For crystals with orthorhombic symmetry or higher, any mode is polarized along one of the mutually perpendicular crystallographic axes, and this means that a field along one of the axes will not produce polarization along the other two. Then, the crystallographic axes are the principal axes of $\chi_{ij}(\omega)$, for any frequency, and we just have to know the components χ_{xx}, χ_{yy}, χ_{zz}.

We will start again from Eqs. (1′) and put the external forces f_ν equal to zero. $\vec{E}$ will be aligned with one of the axes, let us say α, and consequently only the n modes and the electron polarized along α are involved:

$$\ddot{X}_\nu+\gamma_\nu\dot{X}_\nu+\omega_\nu^2X_\nu+\sum_{\mu=1}^{n+1}(\gamma_{\nu\mu}\dot{X}_\mu+\omega_{\nu\mu}^2X_\mu)=Q_\nu E^{\mathrm{tot}}\ . \tag{21}$$

Looking back at the definition of the G matrix, we can write

$$\sum_{\mu=1}^{n+1}G_{\nu\mu}^{-1}(\omega,\infty)X_\mu=Q_\nu E^{\mathrm{tot}}$$

or, in matrix form,

$$\vec{X}=\vec{\vec{G}}(\omega,\infty)\vec{Q}E^{\mathrm{tot}}\ . \tag{22}$$

Consequently,

$$\chi(\omega)=\vec{Q}^{\dagger}\vec{\vec{G}}(\omega,\infty)\vec{Q}\ , \tag{23}$$

so the electric susceptibility is just another quadratic form of the G matrix.

The dielectric function is given by

$$\epsilon_\alpha(\omega)=1+4\pi\vec{Q}_\alpha^{\dagger}\vec{\vec{G}}_\alpha(\omega,\infty)\vec{Q}_\alpha\ , \tag{24}$$

where the index α is now introduced to emphasize that we are talking about the component along the crystallographic axis α.

V. DETERMINATION OF THE PARAMETERS

The parameters involved in the theory are (i) the frequencies ω_ν and linewidths γ_ν of all the modes of a given symmetry, and consequently, a

given polarization; (ii) the reactive ($\omega_{\nu\mu}$) and dissipative ($\gamma_{\nu\mu}$) coupling between all the modes; (iii) the effective charges Q_ν of all the modes; and (iv) n independent Raman amplitudes. We should remember that the total number of modes is $n+1$: n lattice modes and one electronic mode. The total number of parameters is

$$(n+1)(n+3)+n \ .$$

This number is very large even if n is relatively small. For example, for tetragonal $BaTiO_3$, where we have three modes of symmetry A_1; i.e., for $n_z=3$, there are 27 parameters available. The parameters to be determined from infrared reflectivity or Raman scattering can usually be reduced, as discussed below.

For transparent crystals, the frequencies of the electronic modes are far above the frequencies of the lattice modes, by a factor typically in the range 10^1-10^2. This means that unless we have a large first-order coupling between the electrons and phonons, (i) the mutual interferences will be undetectable, and (ii) the indexes of refraction will depend only on the electronic modes. The dielectric function in the visible will be given by

$$\epsilon_\alpha^\infty = 1+4\pi Q_\alpha^2/\omega_\alpha^2 \tag{25a}$$

or

$$Q_\alpha = \left[\frac{\epsilon_\alpha^\infty - 1}{4\pi}\right]^{1/2} \omega_\alpha \ . \tag{25b}$$

The effects of the damping are already negligible in the visible (this is why the crystal is transparent) and, with more reason, in the infrared. ω_α is to be taken as the edge of the absorption band for light with α polarization. So, it is a good approximation to take the electronic modes as undamped oscillators with no first-order coupling with the phonons. The frequencies and effective charges of these oscillators are obtained from measurements at visible and uv frequencies. Now, we are left with $n(n+3)$ parameters, 18 for the A_1 modes of $BaTiO_3$.

Part of these parameters can be determined by the measurement of the reflectivity in the infrared. The normal reflectivity is given by the textbook formula

$$R(\omega) = \frac{|[\epsilon(\omega)]^{1/2}-1|^2}{|[\epsilon(\omega)]^{1/2}+1|^2} \ . \tag{26}$$

Although being a real function, $R(\omega)$ gives complete information about $\epsilon(\omega)$, owing to the Kramers-Kronig relations. However, the set of parameters which can define a given spectrum of $R(\omega)$ is not uniquely defined. In fact, the orthogonal transformation

$$\vec{Q}' = \overleftrightarrow{U}\vec{Q} \ , \tag{27}$$

$$\overleftrightarrow{G}'(\omega,\infty) = \overleftrightarrow{U}\,\overleftrightarrow{G}(\omega,\infty)\,\overleftrightarrow{U}^\dagger \tag{28}$$

will not change the dielectric function. As the only *a priori* condition is that we do not want the electronic mode to couple with the phonons, there is complete freedom to rotate the space of the n lattice modes. The set of all the n-dimensional orthogonal matrices has $\frac{1}{2}n(n-1)$ independent parameters, which means that we have $\frac{1}{2}n(n-1)$ more parameters than the minimum required to fit the data. Looking at the matrix $G^{-1}=(G^{-1})'+i(G^{-1})''$, we can see, in another way, the same number of surplus parameters. As $(G^{-1})'$ and $(G^{-1})''$ are both symmetric and real, we can diagonalize either of them by an orthogonal transformation. However, because $(G^{-1})'$ and $(G^{-1})''$ do not commute (if they did, the system could be entirely decoupled), they cannot be diagonalized simultaneously. So, we can choose to have either pure-real or pure-imaginary coupling for all the modes, and then have $\frac{1}{2}n(n-1)$ less parameters than before. The same kind of discussion can be held about the Raman spectrum of the large-wave-vector TO phonons by just substituting $\vec{\beta}$ for $\vec{Q}$. The G matrix can be split according to

$$\overleftrightarrow{G}^{-1}(\omega,q) = \overleftrightarrow{G}^{-1}(\omega,\infty) - \Phi(\omega,q)\vec{Q}\vec{Q}^\dagger \ . \tag{29}$$

$\overleftrightarrow{G}^{-1}(\omega,\infty)$, and then also $\overleftrightarrow{G}(\omega,\infty)$, does not contain the charges. The spectrum of the large-wave-vector TO modes is

$$S(\omega) \sim \vec{\beta}^\dagger \overleftrightarrow{G}(\omega,\infty)\vec{\beta} \ , \tag{30}$$

which is invariant to

$$\vec{\bar{\beta}} = \overleftrightarrow{U}\vec{\beta} \ ,$$

$$\overleftrightarrow{\bar{G}}(\omega,\infty) = \overleftrightarrow{U}\,\overleftrightarrow{G}(\omega,\infty)\,\overleftrightarrow{U}^\dagger \ .$$

These invariances of the functions $\epsilon(\omega)$ and $S(\omega)$ led the previous investigators to conclude that all the representations obtained by UT are equivalent. However, this is not generally true for modes which are infrared active. In fact, the transformation of the effective charges expressed in Eqs.

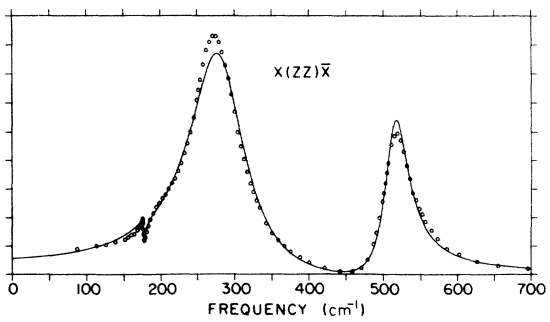

FIG. 1. (ZZ) spectrum of the A_1(TO) phonons in the tetragonal $BaTiO_3$. The continuous line is the best fit to the experiment.

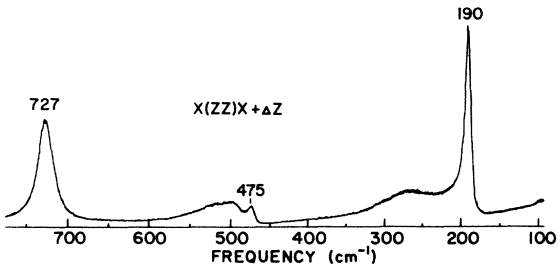

FIG. 2. (ZZ) spectrum of the A_1(LO) phonons in tetragonal $BaTiO_3$. The broad features around 270 and 520 cm^{-1} apparently are the A_1(TO) phonons scattered by the fraction of laser light which is reflected at the exit surface of the crystal.

(11c) and (27) are not compatible with the transformation of the G matrix, except in the particular cases previously discussed. Then we can conclude that there is only one representation in which all the observable quantities of the system fit consistently into the same description.

VI. APPLICATION TO TETRAGONAL $BaTiO_3$

Numerical calculations on the line shape of light scattering by polaritons with A_1 symmetry in $BaTiO_3$ were performed for the two extreme representations of the system: the representation in which the couplings are real and that in which the couplings are pure imaginary. The parameters ω_ν, $\omega_{\nu\mu}$, γ_ν, $\gamma_{\nu\mu}$, and β_ν were obtained from the fitting of the spectrum $x(zz)\bar{x}$. This spectrum with the best theoretical fit, is shown in Fig. 1. We did the fitting for both pure real and pure imaginary couplings. The coupling between the middle and highest polaritons was much larger than that between the lowest and the middle ones, although this last coupling gives origin to more line asymmetries. The coupling between the lowest and the highest was fixed at the value zero, to allow less fitting parameters; this is a reasonable approximation because they are too far from each other, having no spectral superimposition. When we rotate the matrix with real coupling to obtain another matrix with imaginary coupling, we will obtain, in general, a finite imaginary coupling parameter γ_{13} even if we start from ω_{13} equal to zero; but that number (γ_{13}) proved to be very small. As a consequence, even after the approximation above, both representations gave the same fit to the data.

The charges Q_1, Q_2, and Q_3 were calculated from the zeros of the dielectric function. The complex zeros of that function must be the complex frequencies of the longitudinal-optical modes. Figure 2 shows the spectrum of the A_1(LO) phonons. The broad bands around 270 and 520 cm^{-1} have every indication of being the A_1(TO) which appear because of the back reflection of the laser at the exit surface of the crystal. The three A_1(LO) were assigned to the three peaks at 190, 475, and 717 cm^{-1}. As the peaks are sharp, the imaginary part of the frequencies was neglected, and the three charges were calculated from the set of equations

$$\epsilon'(\omega_\nu^L) = 0\,, \quad \nu = 1, 2, 3 \tag{31}$$

where $\epsilon'(\omega)$ is the real part of the function given by Eq. (25). The charge of the electronic oscillator was calculated from the value of the high-frequency dielectric function $\epsilon_z^\infty = 5.07$. All the oscillator parameters are shown in Table I for both representations. The parameters β_ν and Q_ν were transformed to the more practical forms

$$\chi_\nu = (\beta_\nu/\omega_\nu)^2$$

$$S_\nu = (4\pi)^{1/2} Q_\nu (V\omega_\nu^2)^{-1/2} = (4\pi)^{1/2} Z_\nu (VM_\nu\omega_\nu^2)^{-1/2}\,.$$

We included in Table I the infrared strengths calculated by Pinczuk *et al.*,[13] without considering the coupling.

One clear thing in the table is that with imaginary coupling, the frequencies and linewidths of the phonons are close to what we would guess just by visual examination of the spectrum. This is reasonable because of the following: The imaginary coupling is zero at zero frequency, as in fact required by Kramers-Kronig analysis. This means that if the Lyddane-Sachs-Teller (LST) relation is to work, the uncoupled complex frequen-

TABLE I. Parameters associated with the zone-center A_1(TO) phonons in tetragonal $BaTiO_3$. The parameters ω_ν, γ_ν, $\omega_{\nu\mu}$, and $\gamma_{\nu\mu}$ are measured in cm^{-1}; the parameters χ_ν have arbitrary units and S_ν are pure numbers.

	γ_1	ω_1	γ_2	ω_2	γ_3	ω_3	γ_{12}	ω_{12}	γ_{23}	ω_{23}
real coupling	2.0	179	126.5	368	5.5	463	0	82.7	0	294
imag. coupling	3.2	177	89.7	283	40.6	520	12.2	0	54.5	0
		χ_1		χ_2		χ_3	S_1		S_2	S_3
real coupling		0.48		17.9		0.22	1.55		−3.89	0.473
imag. coupling		0.039		17.8		3.9	2.29		−4.34	1.15
Pinczuk *et al.*		**		**		**	2.78		4.63	1.00

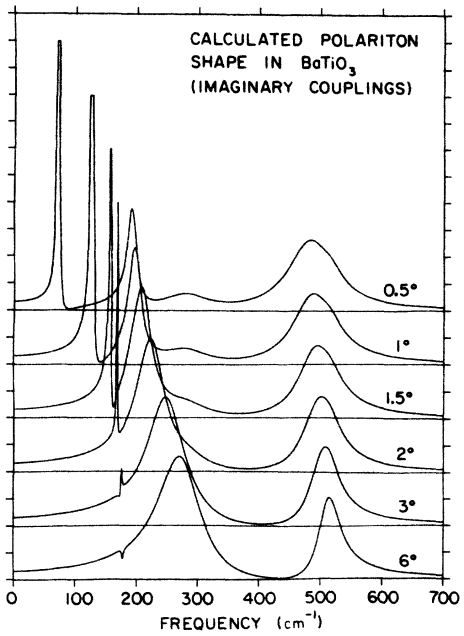

FIG. 3. Calculated shape of the polaritons with A_1 symmetry in tetragonal $BaTiO_3$. Model of real coupling.

cies of the phonons in that representation must be the complex poles of the dielectric constant. The oscillator charges in the model of imaginary coupling are also very close, in absolute values, to what was obtained by Pinczuk *et al.* However, when the coupling is neglected, one can never know the relative sign of those charges.

The representation in which the couplings are real gives a completely different description of the situation: The crystal has only one mode with high intrinsic damping, the one which peaks at 270 cm^{-1}. The highest mode becomes broad because of the huge coupling that it has with the damped mode; this coupling causes also a very large repulsion between the two highest modes. Figures 3 and 4 show the polariton shapes calculated with the parameters of Table I for real and imaginary coupling, respectively. In the calculations, the corrections due to the reflection of the laser at the exit surface of the crystal were made, so that a fraction of the large-angle spectrum stays there for all angles. The polariton shapes are different for real and imaginary couplings, and both fail miserably on predicting the broadening of the lowest polariton at small scattering angles. It becomes very clear that a damping of the form $-i\omega\gamma$, γ being a constant, is not a good description for that polariton when it shifts to smaller frequencies. Part of the observed broadening is due to the finite solid angle of scattering involved in the experiments, but these effects account for less than 20% of the experimental linewidth of the lowest polariton. The increased damping can result from two different sources. One is the different two-phonons background felt by the polariton when its frequency goes toward zero. The most general dependence which γ can have with ω is of the form

$$\gamma=\gamma_0(1+a\omega^2+b\omega^4+c\omega^6+\cdots)\,. \tag{32}$$

In order to explain the observed linewidths, we must assume that the function inside the parentheses has a peak in the region below 150 cm^{-1}, or that it is a monotonically decreasing function of ω. This view finds some support in the fact that the lowest E(TO), whose real frequency is 36 cm^{-1}, is overdamped, having a damping constant γ equal to 90 cm^{-1}. However, the frequency dependence suggested by Benson and Mills,[18] $\gamma=\gamma_0/\omega$, cannot be accepted, because the resulting dielectric function would not obey the Kramers-Kronig relations. The other possible explanation for the broadening is the probable dependence that the damping of a wave packet in an imperfect crystal has with the group velocity of the wave. The observed linewidths can be explained if we assume that γ is frequency independent but varies with the group velocity according to

$$\gamma=\gamma_0+\alpha\frac{1}{c}\frac{\partial\omega}{\partial k}\,, \tag{33}$$

where γ_0 is the very small damping of the corre-

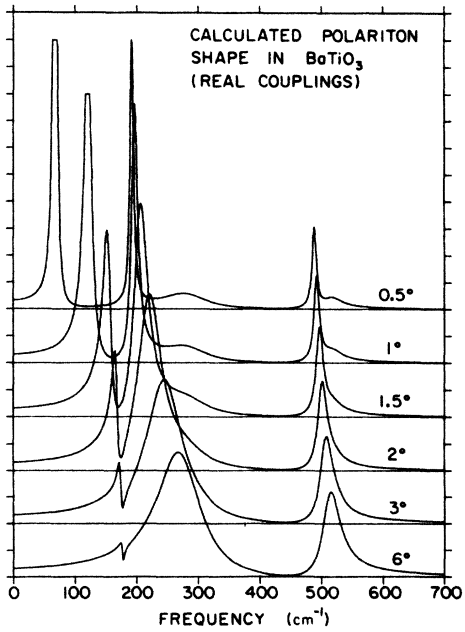

FIG. 4. Calculated shape of the polaritons with A_1 symmetry in tetragonal $BaTiO_3$. Model of imaginary coupling.

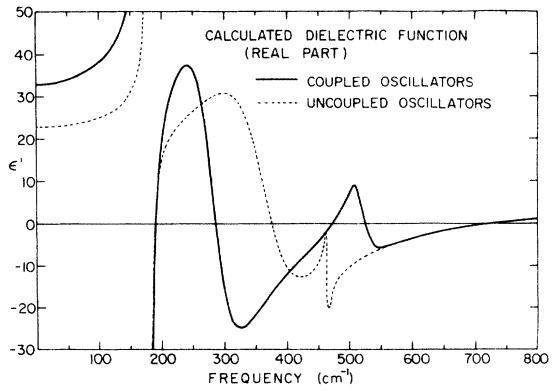

FIG. 5. Calculated dielectric function of tetragonal $BaTiO_3$ along the ferroelectric axis. Real part.

sponding A_1(TO). The constant α would be about 10^3 cm^{-1}. From this value we see that the quasiparticle associated with the lowest polariton would have a mean free path of about 20 μm, independent of the frequency. In this model, the decay of the lowest polariton is due primarily to defects in the crystal, for instance the ferroelectric domain walls, Even if $BaTiO_3$ crystals do not have orthogonal domains, their structure is apparently composed of a set of antiparallel needle-shaped domains along the ferroelectric axis. As the A_1-symmetry polaritons travel necsssarily in the xy plane, they can be badly distrubed by the domain walls. In the model of Comes *et al.*, the chain structure of the polarization correlation is what causes the anisotropic diffuse scattering of x rays and thermal neutrons discussed in Sec. I.

The representation in which the couplings are real gives a picture of the polariton shapes which is closer to the experimental facts, in all respects. The important features of the interference are reasonably well explained by taking real couplings. It fails, however, to give the correct intensity for the polariton corresponding to the A_1(TO) at 520 cm^{-1}, at very small angles. It should be weaker, due to the low intensity of the A_1(LO) at 475 cm^{-1} shown in Fig. 2. However, the imaginary coupling fails even more remarkably on predicting the behavior of that polariton. As a conclusion, it seems to us that purely real coupling is a more successful assumption than pure imaginary coupling and, consequently, the more important part of the complex coupling in barium titanate is its real component. Another fact favoring the assumption of real coupling is the behavior of the parameters when they were free to fit the data. The variation of the coupling parameters with the scattering angle is shown in Ref. 17; the imaginary coupling changed notably with the varying scattering angle, while the real coupling stayed quite stable all the time.

The dielectric function shown in Figs. 5 and 6 was drawn using real coupling. The imaginary part of the dielectric function is, as it should be, a function very similar to the Raman spectrum of the transversal modes, disregarding the obvious changes which result from the difference between the Raman and infrared strengths. For instance the shoulder seen in the Raman scattering of A_1(TO), around 200 cm^{-1}, does not appear in the function $\epsilon''(\omega)$ because the effective charges of the lowest and the middle modes have opposite signs. After we decouple the modes, the middle pole of ϵ becomes even broader than before and the highest pole becomes beautifully sharp, and they shift toward each other. It is clear that the coupling has a much bigger effect on the second and third poles than on the first one.

The low-frequency value of the dielectric function, $\epsilon_0 = 32.9$, (see Fig. 5) agrees very well with the value 33 ± 3 obtained from the slope of the lowest polariton branch; it is amazing to see that one-third of that value is due to the coupling between the phonons, for after we decouple them the value of low-frequency dielectric constant decreases to only 23. However, both values are much lower than the low-frequency value of ϵ obtained by capacitance measurements. Wemple *et al.*[20] reported the value 80 for the dielectric constant along the ferroelectric axis at 250 MHz. The frequency of the measurement was high enough to eliminate any effect due to the piezoelectric resonances.

Once the dielectric function is known, we can calculate the normal incidence reflectivity of the crystal in the infrared; the resulting curve is shown in Fig. 7. The discrepancy between our calculation and the measurements by Spitzer *et al.*,[21] Ikegami *et al.*,[22] Ballantyne,[23] and Barker[24] is radical. However, the significance of this de-

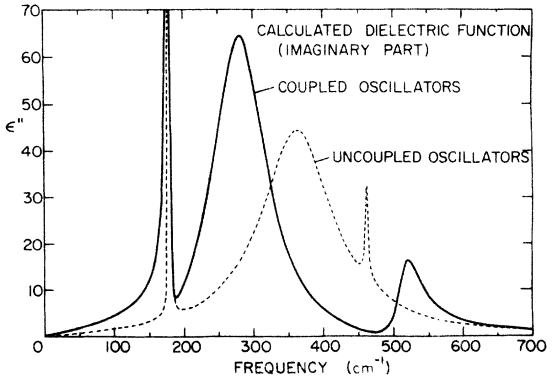

FIG. 6. Calculated dielectric function of tetragonal $BaTiO_3$ along the ferroelectric axis. Imaginary part.

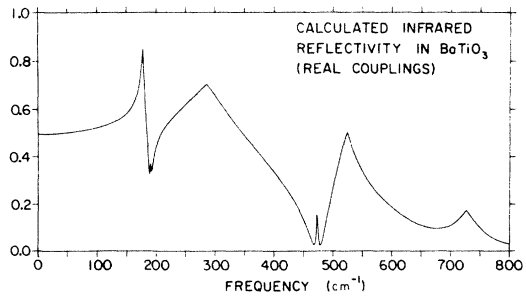

FIG. 7. Normal-incidence reflectivity in tetragonal $BaTiO_3$ for infrared light polarized along the ferroelectric axis.

parture is questionable. All those works, except that of Spitzer *et al.*, were performed on multiple domain samples and, consequently, do not discriminate between A_1 and E modes. Surprisingly enough, Spitzer and co-workers also could not detect any change of the reflectivity for light polarization parallel to and perpendicular to the ferroelectric axis; based on the marked distinctions in the properties of the A_1 and E phonons, one should expect very noticeable differences between these two spectra. However, the differences do not exist and, in fact, the spectrum by Spitzer *et al.* differs from the measurements on ceramic performed by Ikegami *et al.* only in the details of a sharp resonance at about 180 cm^{-1}.

The skin depth of the infrared light below 600 cm^{-1} in $BaTiO_3$ is very small, owing to the large imaginary component of the dielectric function in that region. From Fig. 6, we see that light polarized along z does not penetrate more than a few microns, for most of the frequencies below 600 cm^{-1}. The penetration depth of light polarized in the xy plane should be even smaller, due to the overdamped E(TO), which has a huge infrared strength. Consequently, the properties of the crystal surface are more important than the bulk on determining the characteristics of the reflectivity spectrum, and any surface damage resulting from the sample preparation is expected to affect strongly the measurements; in $BaTiO_3$, the ferroelectric order near the surface of the sample is especially vulnerable; we discovered from some unfortunate experiences in our work, that apparently minor things, such as the thermal shock caused by the fast evaporation of volatile liquids when cleaning the crystal, would damage its surface.

One striking point on the Raman spectrum of the phonons of A_1 symmetry is their qualitative dependence on the polarizability element. It is commonly believed that no change other than alterations of the relative Raman strengths of the modes can appear when one selects different polarizability elements of the same phonons. The changes of the strengths occur because different electrons participate in the Raman process for different tensor elements. In barium titanate, however, when one goes from α_{zz} to α_{xx} the interference shapes change completely. The middle A_1(TO) now peaks at 287 cm^{-1} (instead of 270 cm^{-1}), and stops interfering with the lowest mode. The polariton shapes, probed at the element α_{xx}, are shown in Fig. 8 for a few scattering angles. At small angles such a change would be easier to understand because of the birefringence of the crystal. The electronic modes polarized along the two directions have different charges, which could affect the polariton shapes; even this effect could hardly occur in $BaTiO_3$, because ϵ_0 is much larger than ϵ_∞, which ascribes little importance to the electronic modes in the determination of the polariton curves. We can think of two effects that could result in those changes. One is a very large first-order coupling between electron and phonons. Because different electrons are involved in the Raman events described by the two tensor elements, that kind of coupling could give origin to important changes in the spectra. However, the coupling parameters able to explain the observed changes have to be extremely large. Another possible explanation is to suppose that in $BaTiO_3$ we have interference between the phonons and the second-order background, in addition to the phonon-phonon interferences. As the second-order background looks very different for the polarizations zz and xx, important differentiations in those two spectra could be expected. The second-order scattering becomes more prominent in the spectra of Fig. 8 than in that of Fig. 1 both because of its absolute enhancement and because the A_1(TO) phonons are about three times

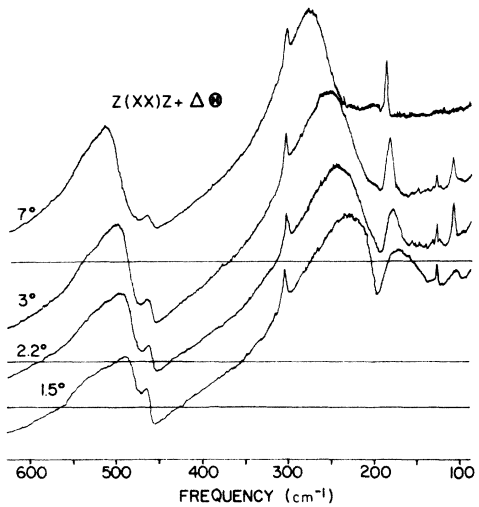

FIG. 8. (XX) spectrum of the polaritons with A_1 symmetry in tetragonal $BaTiO_3$.

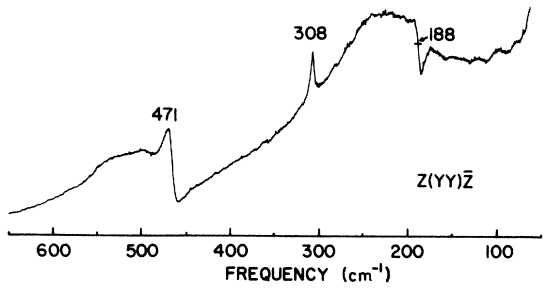

FIG. 9. (XX) spectrum of the A_1(LO) phonons in tetragonal $BaTiO_3$.

weaker in xx than in zz. As we do not know the shape of the second-order background, no attempt was made to fit the spectra of Fig. 8.

One good demonstration of the interaction between the phonons and the second-order continuum is given by the spectrum $Z(YY)\bar{Z}$ shown in Fig. 9. This spectrum should give only the phonons A_1(LO) and the phonon B_1, which is the peak at 308 cm^{-1}; however, the second-order background is present and shows strong interference with the A_1(LO) phonons. We believe that this interaction causes the differences between the polariton shapes at (ZZ) and (XX) polarizations.

To conclude, let us summarize some important results of our work. The main features of the near-forward Raman scattering in $BaTiO_3$, such as the dispersion of the frequencies and the shape of the interferences, can be well explained by the theory of coupled polaritons. All the parameters appearing in the formalisms were evaluated from the A_1(TO) and A_1(LO) spectra, so that no adjustable parameters were available when performing the calculations of the polariton shapes. However, the observed damping of the lowest polariton was much larger than the prediction of the theory; the effect was interpreted as due to the chain structure of the polarization correlation of the crystal. The short correlation length for directions perpendicular to the ferroelectric axis was thought to limit the mean free path of the polariton quasiparticles to values of about 20 μm. This effect, in itself, does not give conclusive support to the disorder model postulated by Comes *et al.*, because the dynamical disorder due to the overdamped E mode could apparently result in the same effect; thus, the double interpretation applied to the anisotropic diffuse scattering of x rays, electrons, and neutrons stays unsolved. However, the discrepancy between the "LST value" of the dielectric constant and the value obtained by capacitance measurements is to be considered a strong argument favoring the hypothesis of site disorder by Comes *et al.* The LST value of ϵ, considering correctly the phonon-phonon coupling, is 33, as we can see in Fig. 5; this value agrees perfectly with that obtained from the slope of the lowest polariton at $k = 0$. Then, to explain the high value of ϵ obtained electrically, we must assume the existence of some extra pole in ϵ at microwaves or below.[25] The overdamped E(TO) cannot contribute to ϵ along the ferroelectric axis, but the tunneling of the Ti ions between the possible sites obviously can generate the missing step in that function.

Another fact favoring the disorder model is the permanence of the broad bands in the paraelectric phase of the crystal. The agreement of the forward scattering with the polariton theory shows conclusively that the broad bands are first-order scattering and consequently should disappear above 130 °C as the crystal assumes the O_h^1 symmetry. The tunneling of the Ti could explain the permanence of part of the spectrum in the paraelectric phase, because according to this model the crystal has O_h symmetry only on the average; the instant symmetry of the unit cell is C_{3v} and if the relaxation time is larger than the times involved in the Raman process, the scattering would be allowed.

Our analysis of the polariton shapes allowed us to conclude that the coupling of the vibrational modes is predominantly real; the model of real coupling explained satisfactorily most of the characteristics of the spectra, while the model of pure imaginary coupling failed completely to explain the shape of the interferences and the small damping of the LO modes. The possibility of discriminating between the two models contradicts the conclusion of the previous investigators that the two models are physically equivalent.

Further investigation of the mechanism of the phase transitions of $BaTiO_3$, particularly the one at 130 °C is desirable. An interesting program is to obtain the phonon contribution to ϵ as a function of the temperature, either by a complete analysis of the function $\epsilon(\omega)$ or by just measuring the slope of the lowest polariton at $k = 0$. It is expected that the disagreement with the electrical measurements will increase as we approach the critical temperature. A quantitative, theoretical analysis of the integrated Raman cross section of the A_1 modes in the presence of the tunneling of the Ti ions could also shed light on the high-temperature behavior of the crystal.

ACKNOWLEDGMENTS

The authors wish to thank the National Science Foundation for their support throughout the course of this work. We would also like to thank Dr. Joel Cherlow for his numerous suggestions which improved this paper.

*Present address: Instituto de Fisica, U. F. M. G., Belo Horizonte, M. G. 30000, Brasil.
†Present address: Instituto de Fisica, Universidade Estadual de Campinas, Campinas, S. P. 13 100, Brasil.

[1]A. S. Barker, Jr. and J. J. Hopfield, Phys. Rev. 135, 1732A (1964).
[2]D. L. Rousseau and S. P. S. Porto, Phys. Rev. Lett. 20, 1354 (1968).
[3]J. F. Scott, Phys. Rev. Lett. 21, 907 (1968).
[4]J. F. Scott, Phys. Rev. Lett. 24, 1107 (1970).
[5]A. Zawadowski and J. Ruvalds, Phys. Rev. Lett. 24, 111 (1970).
[6]R. S. Katiyar, J. F. Ryan, and J. F. Scott, *Light Scattering in Solids* (Fammarion, Paris, 1971).
[7]P. D. Lazay and P. A. Fleury, Phys. Rev. Lett. 26, 1331 (1971).
[8]V. Dvorak, Phys. Rev. 167, 525 (1968).
[9]J. Harada, J. D. Axe and G. Shirane, Phys. Rev. 4, B155 (1971).
[10]J. L. Parsons and L. Rimai, Solid State Commun. 5, 423 (1967).
[11]M. DiDomenico, Jr., S. H. Wemple, S. P. S. Porto, and R. P. Bauman, Phys. Rev. 174, 522 (1968).
[12]W. G. Nilsen and J. G. Skinner, J. Chem. Phys. 47, 1413 (1967); 48, 2240 (1968).
[13]A. Pinczuk, E. Burstein, and S. Ushioda, Solid State Commun. 7, 139 (1969).
[14]G. Shirane, J. D. Axe, J. Harada, and A. Linz, Phys. Rev. B 2, 3651 (1970).
[15]R. Comes, M. Lambert, and A. Guiner, Solid State Commun. 6, 715 (1968).
[16]A. Huller, Solid State Commun. 7, 589 (1969).
[17]A. Chaves, P. da R. Andrade, R. S. Katiyar, and S. P. S. Porto, Nuovo Cimento (to be published).
[18]H. J. Benson and D. L. Mills, Solid State Commun. 8, 1387 (1970).
[19]K. Huang, Proc. R. Soc. A 208, 352 (1951).
[20]S. H. Wemple, M. DiDomenico, Jr., and I. Camlibel, J. Phys. Chem. Solids 29, 1797 (1968).
[21]W. G. Spitzer, Robert C. Miller, D. A. Kleinman, and L. E. Howarth, Phys. Rev. 126, 1710 (1962).
[22]S. Ikegami, I. Ueda, and S. Kisaba, J. Phys. Soc. Jap. 17, 1210 (1962).
[23]Joseph M. Ballantyne, Phys. Rev. 136, A429 (1964).
[24]A. S. Barker, Jr., Phys. Rev. 145, 391 (1966).
[25]A. Chaves and S. P. S. Porto, Solid State Commun. 13, 865 (1973).